SIMULTANEOUS NONLOCAL SELF-SIMILARITY PRIOR FOR IMAGE DENOISING

Zhiyuan Zha[1,3], Xin Yuan[2], Bihan Wen[3], Jiachao Zhang[4], Jiantao Zhou[5] and Ce Zhu[1,]*

[1]School of Information and Communication Engineering,
University of Electronic Science and Technology of China, Chengdu, 611731, China.
[2]Nokia Bell Labs, 600 Mountain Avenue, Murray Hill, NJ, 07974, USA.
[3]School of Electrical and Electronic Engineering, Nanyang Technological University, 639798, Singapore.
[4] Kangni Mechanical and Electrical Institute, Nanjing Institute of Technology, Nanjing 211167, China.
[5]Department of Computer and Information Science, University of Macau, Macau 999078, China.

ABSTRACT

Nonlocal image representation has achieved great success in various image processing tasks such as image denoising, image deblurring and image deblocking. Particularly, by exploiting the image nonlocal self-similarity (NSS) prior, many nonlocal similar patches can be searched across the whole image for a given patch, which has significantly boosted the performance of image restoration. To the best of our knowledge, most existing methods only consider the NSS prior of the input degraded image, while few methods exploit the NSS prior from external clean image corpus. However, how to utilize the NSS priors of input degraded image and external clean image corpus simultaneously is still an open problem. In this paper, we propose a novel approach for image denoising, which exploits simultaneous nonlocal self-similarity (SNSS) by integrating the NSS priors of both the input degraded image and external clean image corpus. Firstly, we search and group nonlocal similar patches from a clean image corpus, and a group-based Gaussian Mixture Model (GMM) learning algorithm is developed to learn an external NSS prior. Then, an optimal group is selected from the best suitable Gaussian component for a group of the noisy image. By integrating the group of the noisy image and the corresponding group of the Gaussian component with a low-rank constraint, an iterative algorithm is developed to solve the proposed SNSS model. Experimental results demonstrate that the proposed SNSS-based denoising method produces superior results compared with many state-of-the-art denoising methods in both objective and perceptual quality.

Index Terms— Image denoising, simultaneous nonlocal self-similarity, gaussian mixture model, low-rank.

1. INTRODUCTION

Image denoising is an old-line problem in the field of image processing, which has still attracted keen interests for researchers of different areas due to its practical significance [1–28]. The goal of image denoising is to recover the original image $\boldsymbol{x}$ from its noisy observation $\boldsymbol{y}$ as precisely as possible, while preserving important details such as edges and textures. The degradation model for image denoising can be mathematically modeled as $\boldsymbol{y} = \boldsymbol{x} + \boldsymbol{n}$, where $\boldsymbol{n}$ is usually assumed to be additive white Gaussian noise. Evidently, image denoising is an ill-posed inverse problem, it is critical to employ the prior knowledge of the original image $\boldsymbol{x}$ so that we can regularize the solution space more feasible and finally obtain high-quality denoised image. To tackle this ill-posed inverse problem, numerous image prior models have been proposed in the past few decades, including transform based methods [1–5], sparse coding based methods [6–8] and nonlocal self-similarity based methods [9–23], etc.

Transform based methods assume that natural images can be sparsely represented by some fixed basis (*e.g.*, DCT and wavelet). Inspired by this, various wavelet shrinkage based methods have been proposed [1–3]. For instance, Chang *et al*. [1] modeled the wavelet transform coefficients as a generalized Gaussian distribution. Portilla *et al*. [2] utilized the scale mixtures of Gaussian in the wavelet domain for image denoising. Though wavelet-based methods present remarkable performance in de-correlation for image signals, these methods sometimes occur noise residuals and artifacts in the denoised image owing to unproper wavelet basis selected. Another well-known transform based method is total variation (TV) [4, 5], which assumes that image gradients obey Laplacian distribution. TV-based methods have shown promising performance in noise remove, while they are apt to over-smooth the images.

Instead of modeling image statistics in transform domains (*e.g.*, wavelet domain and gradient domain), another approach is to model the prior on image patches. One representative work is sparse coding based method [6–8], which assumes that each patch of an image can be represented as a linear combination of a subset of bases from a dictionary. The well-known dictionary learning method, K-SVD has demonstrated promising performance in various applications, ranging from image denoising to computer vision [7, 29, 30]. Considering that natural images are non-Gaussian and image patches are regarded as samples of a multivariate vector, Gaussian mixture model (GMM) has emerged as favored prior for natural image patches [24–27, 31]. For instance, Zoran *et al*. [24] utilized GMM model to learn image patches from natural images and recovered the denoised image through maximizing the expected patch log likelihood (EPLL). Niknejad *et al*. [26] recovered the clean image by using GMM model with spatially constraint patch clustering.

Inspired by the invention of nonlocal means (NLM) denoising [9], perhaps the most remarkable property of natural images is nonlocal self-similarity (NSS) prior [10–23], which characterizes the repetitiveness of textures and structures globally position in images. The NSS-based methods have achieved better empirical results comparing to some local regularization methods. One of the most successful NSS-based methods is BM3D [10], which exploited the NSS prior by constructing 3D arrays and tackled these arrays through sparse collaborative filtering. Mairal *et al*. [13] further generalized the idea of NSS by learning simultaneous sparse coding (LSSC) to achieve impressive denoising performance. Zhang *et al*. [12] pro-

* Corresponding Author.

posed a group-based sparse representation method for image restoration. Xu *et al*. [15] proposed a patch group based on NSS scheme to learn a NSS prior from natural image groups. Assuming that a data matrix constructed by nonlocal similar patches is of low-rank, low-rank minimization methods [17–22] have achieved state-of-the-art denoising performance.

Most existing methods mentioned above only investigated the NSS prior of the input degraded image, while few methods utilize the NSS prior from external clean image corpus. However, how to exploit the NSS priors of input degraded image (Internal) and clean image corpus (External) simultaneously is still an open problem. Bearing this in mind, this paper proposes the simultaneous nonlocal self-similarity (SNSS) prior for image denoising. To the best of our knowledge, few works have simultaneously investigated two NSS priors to image restoration. The proposed SNSS is composed of the following steps. Firstly, we extract nonlocal similar patches from a clean image corpus to construct groups, and a group-based Gaussian mixture model (GMM) learning algorithm is developed to learn an external NSS prior. Secondly, we select an optimal group from the best suitable Gaussian component for a group of the noisy image. Thirdly, by integrating the groups of the noisy image and Gaussian component with a low-rank constraint, we develop an iterative algorithm to solve the proposed SNSS-based model. Our experimental results validate that the proposed SNSS-based denoising outperforms many state-of-the-art denoising methods both quantitatively and qualitatively.

2. LEARNING THE NSS PRIOR FROM NATURAL IMAGES

Different from traditional NSS-based image restoration methods, which have only considered a single NSS prior but ignored another one, this paper exploits the NSS priors of input degraded image and external clean image corpus simultaneously for image denoising. We first develop a group-based Gaussian mixture model (GMM) learning algorithm to learn the NSS prior from the groups of a clean image corpus.

2.1. Group Construction

Since the basic unit of the proposed GMM learning algorithm is image group, we will give a brief introduction on how to construct it. Specifically, an image $\boldsymbol{x}$ with size N is first divided into n overlapped patches $\boldsymbol{x}_i$ of size $\sqrt{b}\times\sqrt{b}$, $i = 1, 2, ..., n$; then for each patch $\boldsymbol{x}_i$, its m similar patches are selected from a searching window with $L \times L$ pixels to form a set $\boldsymbol{S}_i$. Following this, all patches in $\boldsymbol{S}_i$ are stacked into a matrix $\boldsymbol{X}_i \in \mathbb{R}^{b\times m}$, *i.e.*, $\boldsymbol{X}_i = \{\boldsymbol{x}_{i,1}, \boldsymbol{x}_{i,2}, ..., \boldsymbol{x}_{i,m}\}$. This matrix $\boldsymbol{X}_i$ consisting of patches with similar structures is thereby called a group, where $\{\boldsymbol{x}_{i,j}\}_{j=1}^{m}$ denotes the j-th patch (column vector) in the i-th group.

2.2. Group-based GMM Learning

As mentioned above, we extract M groups from a given clean image corpus, and denote a group is

$$\boldsymbol{Z}_i = \{\boldsymbol{z}_{i,j}\}_{j=1}^{m}, i = 1, 2, ..., M, \tag{1}$$

where $\boldsymbol{z}_{i,j}$ denotes the j-th similar patch of the i-th group. Considering that GMM model has been successfully exploited to model the image patch or group priors such as EPLL [24] and PGPG [15], in this subsection, we learn a finite GMM over natural image groups $\{\boldsymbol{Z}_i\}$ as an external NSS prior. To be concrete, by invoking GMM learning algorithm, the likelihood of the given groups $\{\boldsymbol{Z}_i\}$ is

$$P(\boldsymbol{Z}_i) = \sum_{k=1}^{K} \pi_k \prod_{j=1}^{m} \mathcal{N}(\boldsymbol{z}_{i,j}|\boldsymbol{\mu}_k, \boldsymbol{\Sigma}_k), \tag{2}$$

where K is total number of mixture components, and the GMM model is parameterized by mean vectors $\{\boldsymbol{\mu}_k\}$, covariance matrices $\{\boldsymbol{\Sigma}_k\}$ and mixture weights of mixture components $\{\pi_k\}$. By assuming that all groups are independent and applying log to the overall objective likelihood function $\mathcal{L} = \Pi_{i=1}^{M} P(\boldsymbol{Z}_i)$, then we maximize it, namely,

$$\ln \mathcal{L} = \sum_{i=1}^{M} \ln \left(\sum_{k=1}^{K} \pi_k \prod_{j=1}^{m} \mathcal{N}(\boldsymbol{z}_{i,j}|\boldsymbol{\mu}_k, \boldsymbol{\Sigma}_k) \right), \tag{3}$$

We then collect three represent parameters $\boldsymbol{\mu}_k, \boldsymbol{\Sigma}_k$ and π_k through $\boldsymbol{\Theta} = \{\boldsymbol{\mu}_k, \boldsymbol{\Sigma}_k, \pi_k\}_{k=1}^{K}$, and $\boldsymbol{\Theta}$ can be learned by using Expectation Maximization algorithm (EM) [15, 24, 25].

Specifically, in the E-step, we calculate the posterior probability for the component k as:

$$P(k|\boldsymbol{z}_{i,j}, \boldsymbol{\Theta}) = \frac{\pi_k \prod_{j=1}^{m} \mathcal{N}(\boldsymbol{z}_{i,j}|\boldsymbol{\mu}_k, \boldsymbol{\Sigma}_k)}{\sum_{l=1}^{K} \pi_l \prod_{j=1}^{m} \mathcal{N}(\boldsymbol{z}_{i,j}|\boldsymbol{\mu}_l, \boldsymbol{\Sigma}_l)}, \tag{4}$$

$$M_k = \sum_{i=1}^{M} P(k|\boldsymbol{z}_{i,j}, \boldsymbol{\Theta}), \tag{5}$$

In the M-step, for each group $\boldsymbol{Z}_i$, we update the model parameters as follows:

$$\pi_k = M_k/M, \tag{6}$$

$$\boldsymbol{\mu}_k = \frac{\sum_{i=1}^{M} \pi_k \sum_{j=1}^{m} \boldsymbol{z}_{i,j}}{\sum_{i=1}^{M} \pi_k}, \tag{7}$$

$$\boldsymbol{\Sigma}_k = \frac{\sum_{i=1}^{M} P(k|\boldsymbol{z}_{i,j}, \Theta) \sum_{j=1}^{m} \boldsymbol{z}_{i,j} \boldsymbol{z}_{i,j}^T}{M_k}, \tag{8}$$

We iterate over the E-Step and M-Step until convergence. For more details about EM algorithm, please refer to [24].

3. SIMULTANEOUS NONLOCAL SELF-SIMILARITY PRIOR FOR IMAGE DENOISING

In this section, we propose a novel SNSS-based method for image denoising. We first introduce how to combine the NSS priors of input degraded image (Internal) and a clean image corpus (External).

3.1. Combine Internal and External NSS Prior

Similar to subsection 2.1, we extract each patch $\boldsymbol{y}_i \in \mathbb{R}^{\sqrt{b}\times\sqrt{b}}$ from the noisy image $\boldsymbol{y} \in \mathbb{R}^N$, and search for its m similar patches to generate n groups, where the size of each group $\boldsymbol{Y}_i$ is $b \times m$, *i.e.*, $\boldsymbol{Y}_i = \{\boldsymbol{y}_{i,1}, \boldsymbol{y}_{i,2}, ..., \boldsymbol{y}_{i,m}\}$. Then, based on the above group-based GMM learning, the best suitable Gaussian component k is selected for each noisy group $\boldsymbol{Y}_i$. Specifically, by assuming that the image is corrupted by the Gaussian white noise with variance ${\sigma_n}^2$, then the covariance matrix of the k-th Gaussian component will translate into $\boldsymbol{\Sigma}_k + {\sigma_n}^2\boldsymbol{I}$, where $\boldsymbol{I}$ is the identity matrix. The selection that $\boldsymbol{Y}_i$ belongs to the k-th Gaussian component can be obtained by the following poster probability,

$$P(k|\boldsymbol{Y}_i) = \frac{\prod_{j=1}^{m} \mathcal{N}(\boldsymbol{y}_{i,j}|\boldsymbol{0}, \boldsymbol{\Sigma}_k + {\sigma_n}^2\boldsymbol{I})}{\sum_{l=1}^{K} \prod_{j=1}^{m} \mathcal{N}(\boldsymbol{y}_{i,j}|\boldsymbol{0}, \boldsymbol{\Sigma}_l + {\sigma_n}^2\boldsymbol{I})}, \tag{9}$$

Through maximizing Eq. (9), the k-th Gaussian component with the highest probability is selected for each group $\boldsymbol{Y}_i$.

Then, based on this noisy group $\boldsymbol{Y}_i$, for each group of the k-th selected Gaussian component, we compute the distance between $\boldsymbol{Y}_i$ and $\boldsymbol{Z}_{k,i}$,

$$k_i = \arg\min_k \|\boldsymbol{Y}_i - \boldsymbol{Z}_{k,i}\|_2, \tag{10}$$

where $\boldsymbol{Z}_{k,i}$ represents the i-th group of the k-th Gaussian component. By computing Eq. (10), the k_i-th group of the k-th Gaussian

component will be selected and assigned to the noisy group $\boldsymbol{Y}_i$. We then combine the noisy group $\boldsymbol{Y}_i$ and clean image group $\boldsymbol{Z}_{k_i}$ to construct a new (expanded) group,

$$\boldsymbol{Y}_{\mathbf{Z}_i} = [\boldsymbol{Y}_i, \boldsymbol{Z}_{k_i}], \tag{11}$$

where the size of $\boldsymbol{Y}_{\mathbf{Z}_i}$ is $b \times 2m$. Obviously, it can be seen that the new construction group $\boldsymbol{Y}_{\mathbf{Z}_i}$ integrates the NSS information of the input degraded image and external clean image corpus simultaneously.

3.2. Low Rank Minimization for Image Denoising

According to Eq. (11), through using the NSS priors of noisy image and clean natural images together, one can observe that each column of Eq. (11) should have similar structures, and thus the matrix $\boldsymbol{Y}_{\mathbf{Z}_i}$ exhibits the low-rank property. Recently, low-rank minimization based methods have achieved great success for various image and video restoration [17–22]. The representative low-rank minimization method, nuclear norm minimization (NNM) [18], has been adopted for video denoising. However, NNM usually tends to overshrink the rank components, and therefore limits its capability and flexibility. Compared with NNM, the weighted nuclear norm minimization (WNNM) [19] assigns different weights to different singular values such that the matrix rank approximation becomes more accurate. In this subsection, inspired by the success of WNNM model for image restoration [3, 19], we develop an iterative algorithm to solve the proposed SNSS with WNNM (SNSS-WNNM) model for image denoising. Specifically, according to degradation model of additive Gaussian noise, we have $\boldsymbol{Y}_{\mathbf{Z}_i} = \boldsymbol{X}_{\mathbf{Z}_i} + \boldsymbol{N}_{\mathbf{Z}_i}$, where $\boldsymbol{X}_{\mathbf{Z}_i}$ and $\boldsymbol{N}_{\mathbf{Z}_i}$ are the group matrices of the original and noise, respectively. Note that, here we only assume the front half of $\boldsymbol{Y}_{\mathbf{Z}_i}$ contains noise, while the whole part of $\boldsymbol{Y}_{\mathbf{Z}_i}$ has a low-rank property. Then, we apply the WNNM model to solve $\boldsymbol{X}_{\mathbf{Z}_i}$ for image denoising, and $\boldsymbol{X}_{\mathbf{Z}_i}$ can be estimated by solving the following optimization problem,

$$\hat{\boldsymbol{X}}_{\mathbf{Z}_i} = \min_{\boldsymbol{X}_{\mathbf{Z}_i}} \left(\tfrac{1}{{\sigma_n}^2} \|\boldsymbol{Y}_{\mathbf{Z}_i} - \boldsymbol{X}_{\mathbf{Z}_i}\|_F^2 + \|\boldsymbol{X}_{\mathbf{Z}_i}\|_{\boldsymbol{w}_i,*} \right), \tag{12}$$

where $\|\boldsymbol{X}_{\mathbf{Z}_i}\|_{\boldsymbol{w}_i,*} = \sum_j w_{i,j}\delta_{i,j}$, $j = \min(b, 2m)$, $\delta_{i,j}$ is the j-th singular value of $\boldsymbol{Y}_{\mathbf{Z}_i}$. $\boldsymbol{w}_i = [w_{i,1}, w_{i,2}, ..., w_{i,j}]$ and $w_{i,j} > 0$ is a non-negative weighted assigned to $\delta_{i,j}$. Obviously, Eq. (12) can be effectively solved by the weighted singular value thresholding algorithm [3]. Let $\boldsymbol{Y}_{\mathbf{Z}_i} = \boldsymbol{U}_i\boldsymbol{\Delta}_i\boldsymbol{V}_i^T$, the closed-form solution of Eq. (12) is given by [3],

$$\hat{\boldsymbol{X}}_{\mathbf{Z}_i} = \boldsymbol{U}_i(\boldsymbol{\Delta}_i - \mathrm{diag}(\boldsymbol{w}_i))_+\boldsymbol{V}_i^T, \tag{13}$$

where $(x)_+ = \max(x, 0)$. For the weight $\boldsymbol{w}_i$ of each group $\boldsymbol{X}_{\mathbf{Z}_i}$, given that fact the singular values have physical meanings of each group, *i.e.*, large singular values of each group usually contain major edge and texture information, we usually shrink large singular values less, while shrinking smaller ones more [3, 19, 32]. In other words, the weight $\boldsymbol{w}_i$ of each group $\boldsymbol{X}_{\mathbf{Z}_i}$ should set to be inverse to the singular values, and therefore, the weight is heuristically set as $w_{i,j} = c/(\delta_{i,j} + \epsilon)$ in [19], where c and ϵ are the constant. However, because of this weight setting, WNNM in [19] sometimes pops out error in the operation of SVD. In order to avoid this error, in this paper we present an adaptive weight setting scheme. To be concrete, inspired by [1, 17, 22], the weight $\boldsymbol{w}_i$ of each group $\boldsymbol{X}_{\mathbf{Z}_i}$ is set as $\boldsymbol{w}_i = c * 2\sqrt{2}{\sigma_n}^2/(\boldsymbol{\gamma}_i + \epsilon)$, where $\boldsymbol{\gamma}_i$ represents the estimated standard variance of the singular values of each group $\hat{\boldsymbol{X}}_{\mathbf{Z}_i}$ in each iteration. Please refer to [1] on the robustness analysis of this weight setting.

Following this, according to the solution of $\hat{\boldsymbol{X}}_{\mathbf{Z}_i}$ in Eq. (13), then the final estimated clean group $\hat{\boldsymbol{X}}_i$ is equal to $\hat{\boldsymbol{X}}_{\mathbf{Z}_i}(:, 1 : m)$. After obtaining all estimated groups $\{\hat{\boldsymbol{X}}_i\}$, we get the full image $\hat{\boldsymbol{x}}$ by putting the groups back to their original locations and averaging the overlapped pixels. In practice, we could perform the above denoising procedure for several iterations to achieve better results. Specifically, in the t-th iteration, the iterative regularization strategy [5] is used to update the estimation of the noise standard variance, *i.e.*, the standard deviation of noise σ_n in the t-th iteration is adjusted as ${\sigma_n}^t = \mu\sqrt{{\sigma_n}^2 - \|\boldsymbol{y} - \boldsymbol{x}^{t-1}\|_2^2}$, where μ is a constant. Furthermore, we choose the following stop criterion of iteration for the proposed denoising algorithm, *i.e.*, $\|\hat{\boldsymbol{x}}^t - \hat{\boldsymbol{x}}^{t-1}\|_2^2/\|\hat{\boldsymbol{x}}^{t-1}\|_2^2 < \rho$, where ρ is a small constant.

Till now, we have been explained the whole procedure of the proposed scheme. The complete description of the proposed SNSS-WNNM for image denoising is provided in Algorithm 1.

Algorithm 1 The Proposed SNSS-WNNM for Image Denoising.

Require: Noisy image $\boldsymbol{y}$ and Group-based GMM learning model.
Initialize $\hat{\boldsymbol{x}}^0 = \boldsymbol{y}$, $\boldsymbol{y}^0 = \boldsymbol{y}$, σ_n, b, c, m, L, K, μ, η, ρ and ϵ.
for $t = 1, 2, ..., Iter$ **do**
  Iterative Regularization $\boldsymbol{y}^t = \hat{\boldsymbol{x}}^{t-1} + \eta(\boldsymbol{y} - \boldsymbol{y}^{t-1})$.
  for Each patch $\boldsymbol{y}_i$ in $\boldsymbol{y}^t$ **do**
    Find nonlocal similar patches to form a group $\boldsymbol{Y}_i$.
    The best Gaussian component is selected by Eq. (9).
    Choosing the optimal group $\boldsymbol{Z}_{k_i}$ for noisy group $\boldsymbol{Y}_i$ by Eq. (10).
    Constructing the new group $\boldsymbol{Y}_{\mathbf{Z}_i}$ by Eq. (11).
    $[\boldsymbol{U}_i, \boldsymbol{\Delta}_i, \boldsymbol{V}_i] = \mathrm{SVD}(\boldsymbol{Y}_{\mathbf{Z}_i})$;
    Estimate the weight $\boldsymbol{w}_i$ by $\boldsymbol{w}_i = c * 2\sqrt{2}{\sigma_n}^2/(\boldsymbol{\gamma}_i + \epsilon)$;
    Get the estimation of $\hat{\boldsymbol{X}}_{\mathbf{Z}_i}$ by Eq. (13);
    Get the estimation: $\hat{\boldsymbol{X}}_i = \hat{\boldsymbol{X}}_{\mathbf{Z}_i}(:, 1 : m)$;
  end for
  Aggregate $\boldsymbol{X}_i$ to form the denoised image $\hat{\boldsymbol{x}}^t$.
end for
Output: The final denoised image $\hat{\boldsymbol{x}}$.

Fig. 1. All test images.

4. EXPERIMENTAL RESULTS

In this section, extensive experiments of the proposed SNSS-WNNM method are conducted for image denoising. We evaluate all competing methods on 12 widely used images shown in Fig. 1. Zero mean additive white Gaussian noises are added to those test images to generate the noisy observations. The source code of the proposed SNSS is available at: https://drive.google.com/open?id=15z6M5dfrxNUm1MFyXI2bofW6xYQMQqAJ.

4.1. Parameter Setting

There are several parameters in the proposed denoising algorithm. In the Group-based GMM learning stage, the training groups used in our experiments were sampled from the Kodak photoCD dataset [1], which includes 24 natural images. We extract each patch in every 10 pixels along both horizontal and vertical directions for an image and construct about 150,000 groups from the Kodak photoCD dataset. The size of each patch $\sqrt{b} \times \sqrt{b}$ is set to be 7×7, 8×8 and 9×9 for

[1] http://r0k.us/graphics/kodak/.

Table 1. PSNR (dB) results of different denoising methods.

	$\sigma_n = 40$										$\sigma_n = 50$									
Images	**BM3D**	**EPLL**	**LPCA**	**Plow**	**NCSR**	**PGPD**	**aGMM**	**OGLR**	**INSS-WNNM**	**SNSS-WNNM**	**BM3D**	**EPLL**	**LPCA**	**Plow**	**NCSR**	**PGPD**	**aGMM**	**OGLR**	**INSS-WNNM**	**SNSS-WNNM**
Airplane	26.88	27.08	26.24	26.70	26.78	27.12	26.95	26.82	27.15	**27.26**	25.76	25.96	25.08	25.64	25.63	25.98	25.83	25.67	26.00	**26.22**
boats	27.76	27.42	26.73	27.55	27.52	27.90	27.60	27.69	27.86	**27.91**	26.74	26.31	25.58	26.38	26.37	26.82	26.50	26.41	26.88	**26.90**
C.Man	27.18	27.03	26.50	26.56	27.10	27.34	26.91	26.93	27.34	**27.45**	26.13	26.01	25.43	25.62	26.13	26.46	25.88	25.93	26.30	**26.61**
Monarch	26.72	26.89	26.06	26.43	26.81	27.02	26.87	27.00	27.27	**27.34**	25.82	25.78	24.76	25.41	25.73	26.00	25.82	25.78	26.17	**26.27**
Foreman	31.29	30.28	30.23	30.90	31.52	31.55	30.95	31.64	31.80	**31.84**	30.36	29.20	28.97	29.60	30.41	30.45	29.80	30.00	**30.87**	30.67
House	30.65	29.89	29.72	30.25	30.79	31.02	30.40	30.68	31.37	**31.46**	29.69	28.79	28.50	28.99	29.61	29.93	29.28	29.17	30.43	**30.47**
Leaves	25.69	25.62	25.02	25.45	26.20	26.29	25.76	26.06	26.97	**26.97**	24.68	24.39	23.48	24.28	24.94	25.03	24.42	24.63	25.61	**25.71**
Lena	27.82	27.78	27.23	27.78	28.00	**28.22**	27.91	28.04	28.07	28.18	26.90	26.68	26.05	26.70	26.94	**27.15**	26.85	26.78	27.12	27.12
Man	25.49	25.63	24.93	25.37	25.40	**25.68**	25.45	25.47	25.54	25.65	24.55	24.70	23.92	24.47	24.46	24.74	24.57	24.44	24.63	**24.78**
Pentagon	25.10	24.79	24.31	25.10	24.93	25.11	24.75	25.14	25.16	**25.22**	24.21	23.83	23.28	24.18	23.94	24.17	23.81	24.13	24.30	**24.37**
Plants	29.14	28.96	28.26	28.90	28.73	29.36	29.12	29.27	29.40	**29.48**	28.11	27.83	27.18	27.75	27.65	28.25	28.00	27.94	28.32	**28.36**
Starfish	26.06	26.12	25.52	25.70	26.17	26.21	26.16	26.00	26.52	**26.54**	25.04	25.05	24.32	24.71	25.06	25.11	25.09	24.84	25.33	**25.46**
Average	27.48	27.29	26.73	27.22	27.50	27.74	27.40	27.56	27.87	**27.94**	26.50	26.21	25.55	26.14	26.40	26.67	26.32	26.31	26.83	**26.91**
	$\sigma_n = 75$										$\sigma_n = 100$									
Images	**BM3D**	**EPLL**	**LPCA**	**Plow**	**NCSR**	**PGPD**	**aGMM**	**OGLR**	**INSS-WNNM**	**SNSS-WNNM**	**BM3D**	**EPLL**	**LPCA**	**Plow**	**NCSR**	**PGPD**	**aGMM**	**OGLR**	**INSS-WNNM**	**SNSS-WNNM**
Airplane	23.99	24.03	23.23	23.67	23.76	24.15	23.95	23.79	24.13	**24.17**	22.89	22.78	22.02	22.30	22.60	**23.02**	22.67	22.31	23.00	22.98
boats	24.82	24.33	23.64	24.23	24.44	24.83	24.51	24.40	24.93	**25.02**	23.47	23.01	22.34	22.69	22.98	23.47	23.14	22.74	23.51	**23.63**
C.Man	24.33	24.18	23.46	23.64	24.20	24.64	24.13	24.00	24.75	**24.86**	23.08	22.84	22.13	22.22	22.91	23.23	22.86	22.50	23.36	**23.38**
Monarch	23.91	23.73	22.41	23.34	23.67	24.00	23.85	23.73	24.37	**24.44**	22.52	22.24	20.79	21.83	22.10	22.56	22.42	21.87	**22.90**	22.79
Foreman	28.07	27.24	26.72	27.15	28.18	28.39	27.67	27.96	28.66	**28.79**	26.51	25.91	25.14	25.55	26.55	26.81	26.20	26.11	27.31	**27.46**
House	27.51	26.70	26.19	26.52	27.16	27.81	27.11	27.10	28.45	**28.62**	25.87	25.21	24.51	24.72	25.49	26.17	25.55	25.07	26.81	**26.97**
Leaves	22.49	22.03	20.83	22.02	22.60	22.61	21.96	22.20	23.39	**23.45**	20.90	20.26	19.13	20.43	20.84	20.95	20.29	20.28	21.74	**21.76**
Lena	25.17	24.75	23.98	24.64	25.02	25.30	25.02	24.90	25.32	**25.37**	23.87	23.46	22.54	23.19	23.63	24.02	23.73	23.18	24.23	**24.30**
Man	23.03	**23.06**	22.16	22.76	22.80	23.09	22.98	22.80	22.90	23.05	22.00	21.97	20.95	21.55	21.68	22.03	21.91	21.40	21.93	**22.05**
Pentagon	22.59	22.18	21.57	22.40	22.04	22.55	22.11	22.58	22.66	**22.69**	21.45	21.12	20.52	21.12	20.92	21.50	21.02	21.16	21.45	**21.65**
Plants	26.25	25.90	25.33	25.57	25.75	26.33	26.05	25.89	26.21	**26.35**	24.98	24.65	24.13	24.14	24.46	**25.06**	24.75	24.30	24.83	24.96
Starfish	23.27	23.17	22.37	22.82	23.18	23.23	23.22	23.00	23.35	**23.42**	22.10	21.92	21.16	21.48	21.91	22.08	21.95	21.52	22.09	**22.17**
Average	24.62	24.28	23.49	24.07	24.40	24.74	24.38	24.36	24.93	**25.02**	23.30	22.95	22.11	22.60	23.00	23.41	23.04	22.70	23.60	**23.67**

$10 < \sigma_n \leq 50$, $50 < \sigma_n \leq 75$ and $50 < \sigma_n \leq 100$, respectively. The number of Gaussian components K is set to 256. The searching window $L \times L$ is set to be 25×25 and the similar patches m is set to 30. In the denoising stage, there are four parameters including η, μ, c and ρ. The parameters (η, μ, c, ρ) are set to (0.1, 0.6, 1.8, 0.0026), (0.1, 0.5, 1.7, 0.0013), (0.1, 0.5, 1.6, 0.0015), (0.1, 0.5, 1.3, 0.0011), (0.1, 0.4, 2, 0.0011), (0.1, 0.5, 1.3, 0.0011) and (0.1, 0.4, 2, 0.0014) for $\sigma_n \leq 10$, $10 < \sigma_n \leq 20$, $20 < \sigma_n \leq 30$, $30 < \sigma_n \leq 40$, $40 < \sigma_n \leq 50$, $50 < \sigma_n \leq 75$ and $75 < \sigma_n \leq 100$, respectively.

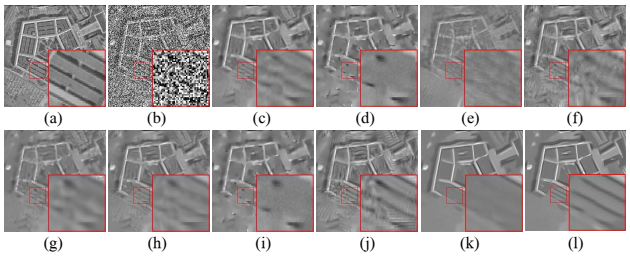

Fig. 2. Denoising results on image *Pentagon* by different methods (noise level σ_n = 100). (a) Original image; (b) Noisy image; (c) BM3D [10] (PSNR = 21.45dB); (d) EPLL [24] (PSNR = 21.12dB); (e) LPCA [14] (PSNR = 20.52dB); (f) Plow [33] (PSNR = 21.12dB); (g) NCSR [11] (PSNR = 20.92dB); (h) PGPD [15] (PSNR = 21.50dB); (i) aGMM [27] (PSNR = 21.02dB); (j) OGLR [34] (PSNR = 21.16dB); (k) INSS-WNNM (PSNR = 21.45dB); (l) SNSS-WNNM (PSNR = **21.65dB**).

4.2. Comparison with State-of-the-Art Methods

In this subsection, we evaluate the effectiveness of the proposed SNSS-WNNM by comparing it with several state-of-the-art denoising methods including BM3D [10], EPLL [24], LPCA [14], Plow [33], NCSR [11], PGPD [2] [15], aGMM [27] and OGLR [34]. Note that, the single nonlocal redundancies are utilized for all competing methods, while two NSS priors together are exploited to the proposed SNSS model. We also compare the proposed SNSS-WNNM with internal NSS-WNNM (INSS-WNNM) method, which selects the similar patches from noisy image as same as the proposed SNSS-WNNM to generate a group and solves it by WNNM [3] algorithm. Due to the page limit, we only present the denoising results at four noise levels, *i.e.*, Gaussian white noise with standard deviations $\{\sigma_n = 40, 50, 75, 100\}$. The PSNR results for all competing methods are shown in Table 1, with the best results highlighted in bold. Obviously, the proposed SNSS-WNNM achieves better results than all competing methods in most cases. It is clear that the proposed SNSS-WNNM consistently outperforms the INSS-WNNM method (the only exception is that the image *Foreman* with $\sigma_n = 50$ and image *Monarch* $\sigma_n = 100$ are slightly better than the proposed SNSS-WNNM). The average gains of the proposed SNSS-WNNM over BM3D, EPLL, LPCA, Plow, NCSR, PGPD, aGMM, OGLR and INSS-WNNM methods are as much as 0.41dB, 0.71dB, 1.42dB, 0.88dB, 0.56dB, 0.25dB, 0.60dB, 0.65dB and 0.08dB, respectively. The visual comparison of image *Pentagon* with $\sigma_n = 100$ is shown in Fig. 2. It can be seen that LPCA, NCSR and INSS-WNNM methods often generate over-smooth effect, while BM3D, EPLL, PLow, PGPD, aGMM and OGLR methods still suffer from some undesirable artifacts. The proposed SNSS-WNNM is able to preserve the fine image details and suppress undesirable artifacts more effective than other competing methods. Therefore, these results validate that the effective and superior of the proposed SNSS model.

[2] A well-known state-of-the-art image denoising method by using external NSS prior.

5. CONCLUSION

We have proposed a novel method for image denoising, termed simultaneous nonlocal self-similarity (SNSS), to exploit the NSS priors in both the degraded image and external clean image corpus. We have first extracted nonlocal similar patches from a clean image corpus to construct groups, and then we have developed a group-based GMM learning algorithm to learn an external NSS prior. Following this, we have selected an optimal group of the best suitable Gaussian component for a group of the noisy image. By integrating the groups of the noisy image and the Gaussian component with a low-rank constraint (*i.e.*, WNNM), we have developed an iterative algorithm to solve the proposed SNSS-WNNM model. Experimental results have demonstrated that the proposed SNSS-WNNM outperforms many state-of-the-art denoising methods in terms of PSNR and visual perception.

6. ACKNOWLEDGE

This work was supported by the NSFC (61571102), the applied research programs of science and technology., Sichuan Province (No. 2018JY0035), the Ministry of Education, Republic of Singapore, under the Start-up Grant and the Macau Science and Technology Development Fund under Grant FDCT/077/2018/A2.

References

[1] S. G. Chang, B. Yu, and M. Vetterli, "Adaptive wavelet thresholding for image denoising and compression," *IEEE transactions on image processing*, vol. 9, no. 9, pp. 1532–1546, 2000.

[2] J. Portilla, V. Strela, M. J. Wainwright, and E. P. Simoncelli, "Image denoising using scale mixtures of gaussians in the wavelet domain," *IEEE Transactions on Image processing*, vol. 12, no. 11, pp. 1338–1351, 2003.

[3] S. Gu, Q. Xie, D. Meng, W. Zuo, X. Feng, and L. Zhang, "Weighted nuclear norm minimization and its applications to low level vision," *International Journal of Computer Vision*, vol. 121, no. 2, pp. 183–208, 2017.

[4] L. I. Rudin, S. Osher, and E. Fatemi, "Nonlinear total variation based noise removal algorithms," *Physica D: nonlinear phenomena*, vol. 60, no. 1-4, pp. 259–268, 1992.

[5] S. Osher, M. Burger, D. Goldfarb, J. Xu, and W. Yin, "An iterative regularization method for total variation-based image restoration," *Multiscale Modeling & Simulation*, vol. 4, no. 2, pp. 460–489, 2005.

[6] M. Elad and M. Aharon, "Image denoising via sparse and redundant representations over learned dictionaries," *IEEE Transactions on Image processing*, vol. 15, no. 12, pp. 3736–3745, 2006.

[7] M. Aharon, M. Elad, and A. Bruckstein, "K-svd: An algorithm for designing overcomplete dictionaries for sparse representation," *IEEE Transactions on signal processing*, vol. 54, no. 11, pp. 4311, 2006.

[8] J. Yang, J. Wright, T. S. Huang, and Y. Ma, "Image super-resolution via sparse representation," *IEEE transactions on image processing*, vol. 19, no. 11, pp. 2861–2873, 2010.

[9] A. Buades, B. Coll, and J. M. Morel, "A non-local algorithm for image denoising," in *Computer Vision and Pattern Recognition, 2005. CVPR 2005. IEEE Computer Society Conference on*. IEEE, 2005, vol. 2, pp. 60–65.

[10] K. Dabov, A. Foi, V. Katkovnik, and K. Egiazarian, "Image denoising by sparse 3-d transform-domain collaborative filtering," *IEEE Transactions on image processing*, vol. 16, no. 8, pp. 2080–2095, 2007.

[11] W. Dong, L. Zhang, G. Shi, and X. Li, "Nonlocally centralized sparse representation for image restoration," *IEEE Transactions on Image Processing*, vol. 22, no. 4, pp. 1620–1630, 2013.

[12] J. Zhang, D. Zhao, and W. Gao, "Group-based sparse representation for image restoration," *IEEE Transactions on Image Processing*, vol. 23, no. 8, pp. 3336–3351, 2014.

[13] J. Mairal, F. Bach, J. Ponce, G. Sapiro, and A. Zisserman, "Non-local sparse models for image restoration," in *Computer Vision, 2009 IEEE 12th International Conference on*. IEEE, 2009, pp. 2272–2279.

[14] B. Wen, S. Ravishankar, and Y. Bresler, "Structured overcomplete sparsifying transform learning with convergence guarantees and applications," *International Journal of Computer Vision*, vol. 114, no. 2-3, pp. 137–167, 2015.

[15] J. Xu, L. Zhang, W. Zuo, D. Zhang, and X. Feng, "Patch group based nonlocal self-similarity prior learning for image denoising," in *Proceedings of the IEEE international conference on computer vision*, 2015, pp. 244–252.

[16] Z. Zha, X. Zhang, Q. Wang, Y. Bai, L. Tang, and X. Yuan, "Group sparsity residual with non-local samples for image denoising," in *2018 IEEE International Conference on Acoustics, Speech and Signal Processing (ICASSP)*, April 2018, pp. 1353–1357.

[17] W. Dong, G. Shi, and X. Li, "Nonlocal image restoration with bilateral variance estimation: a low-rank approach," *IEEE transactions on image processing*, vol. 22, no. 2, pp. 700–711, 2013.

[18] H. Ji, C. Liu, Z. Shen, and Y. Xu, "Robust video denoising using low rank matrix completion," in *2010 IEEE Computer Society Conference on Computer Vision and Pattern Recognition*, June 2010, pp. 1791–1798.

[19] S. Gu, L. Zhang, W. Zuo, and X. Feng, "Weighted nuclear norm minimization with application to image denoising," in *Proceedings of the IEEE Conference on Computer Vision and Pattern Recognition*, 2014, pp. 2862–2869.

[20] Y. Hu, D. Zhang, J. Ye, X. Li, and X. He, "Fast and accurate matrix completion via truncated nuclear norm regularization," *IEEE transactions on pattern analysis and machine intelligence*, p. 1, 2012.

[21] Y. Xie, S. Gu, Y. Liu, W. Zuo, W. Zhang, and L. Zhang, "Weighted schatten p-norm minimization for image denoising and background subtraction," *IEEE transactions on image processing*, vol. 25, no. 10, pp. 4842–4857, 2016.

[22] J. Zhang, R. Xiong, C. Zhao, Y. Zhang, S. Ma, and W. Gao, "Concolor: Constrained non-convex low-rank model for image deblocking," *IEEE Transactions on Image Processing*, vol. 25, no. 3, pp. 1246–1259, 2016.

[23] Q. Wang, X. Zhang, Y. Wu, L. Tang, and Z. Zha, "Nonconvex weighted ℓ_p minimization based group sparse representation framework for image denoising," *IEEE Signal Processing Letters*, vol. 24, no. 11, pp. 1686–1690, 2017.

[24] D. Zoran and Y. Weiss, "From learning models of natural image patches to whole image restoration," in *Computer Vision (ICCV), 2011 IEEE International Conference on*. IEEE, 2011, pp. 479–486.

[25] G. Yu, G. Sapiro, and S. Mallat, "Solving inverse problems with piecewise linear estimators: From gaussian mixture models to structured sparsity," *IEEE Transactions on Image Processing*, vol. 21, no. 5, pp. 2481–2499, 2012.

[26] M. Niknejad, H. Rabbani, and M. Babaie-Zadeh, "Image restoration using gaussian mixture models with spatially constrained patch clustering," *IEEE Transactions on Image Processing*, vol. 24, no. 11, pp. 3624–3636, 2015.

[27] E. Luo, S. H. Chan, and T. O. Nguyen, "Adaptive image denoising by mixture adaptation," *IEEE transactions on image processing*, vol. 25, no. 10, pp. 4489–4503, 2016.

[28] X. Yuan, V. Rao, S. Han, and L. Carin, "Hierarchical infinite divisibility for multiscale shrinkage," *IEEE Transactions on Signal Processing*, vol. 62, no. 17, pp. 4363–4374, 2014.

[29] Budianto and D. P. K. Lun, "Robust fringe projection profilometry via sparse representation," *IEEE Transactions on Image Processing*, vol. 25, no. 4, pp. 1726–1739, April 2016.

[30] Z. Jiang, Z. Lin, and L. S. Davis, "Label consistent k-svd: Learning a discriminative dictionary for recognition," *IEEE transactions on pattern analysis and machine intelligence*, vol. 35, no. 11, pp. 2651–2664, 2013.

[31] J. Yang, X. Yuan, X. Liao, P. Llull, D. J. Brady, G. Sapiro, and L. Carin, "Video compressive sensing using gaussian mixture models," *IEEE Transactions on Image Processing*, vol. 23, no. 11, pp. 4863–4878, 2014.

[32] E. J. Candes, M. B. Wakin, and S. P. Boyd, "Enhancing sparsity by reweighted ℓ_1 minimization," *Journal of Fourier analysis and applications*, vol. 14, no. 5-6, pp. 877–905, 2008.

[33] P. Chatterjee and P. Milanfar, "Patch-based near-optimal image denoising," *IEEE Transactions on Image Processing*, vol. 21, no. 4, pp. 1635, 2012.

[34] J. Pang and G. Cheung, "Graph laplacian regularization for image denoising: Analysis in the continuous domain," *IEEE Transactions on Image Processing*, vol. 26, no. 4, pp. 1770–1785, 2017.